

High Radial Confinement Mode Induced by dc Limiter Biasing in the HIEI Tandem Mirror

O. Sakai, Y. Yasaka, and R. Itatani

Department of Electronics, Kyoto University, Kyoto 606, Japan

(Received 1 December 1992)

A transition from low to high radial confinement mode is triggered by biasing a limiter in the HIEI tandem mirror. Positive dc biasing gives rise to reduction of the fluctuation level in density and potential in the periphery, drop of neutral line emission, and bifurcation in limiter current. After the transition, the plasma exhibits density rise in the bulk and steepening of the density gradient. Significant radial rotational shear is observed when the edge turbulence is suppressed by the biasing. The total feature shows similar characteristics of L - to H -mode transition observed in tokamak devices.

PACS numbers: 52.25.Gj, 52.35.Qz, 52.55.Jd

Since the axial particle confinement in tandem mirrors was greatly improved by forming a confining potential with a thermal barrier [1,2], the radial particle transport has become of primary importance as in tokamaks. The discovery of an improved confinement regime [3], which is called the H mode, has initiated extensive investigations for enhanced radial confinement in many tokamak devices. In H -mode discharges, which are generally generated by high power auxiliary heating, the following features are observed: Transition through bifurcation leads to the drops of H_α/D_α emission, density, and energy rise, and density profile is steepened on the edge. Particle or energy confinement time is enhanced by a factor of 1.5–3 in comparison with L -mode plasmas. The understanding of the conditions leading to the H mode and the physical mechanism of reduction of particle and energy loss are essential in order to produce a controlled improved confinement. Some theoretical and experimental studies have shown that the radial currents/electric fields could trigger the H mode through sheared plasma rotation [4–7]. Although no observation of H -mode-like behavior has been reported in tandem mirror devices, similar situations could be realized through the generation of radial electric field E_r and/or its shear.

Earlier work on mirror devices has shown the possibilities of control of radial electric fields and reduction of fluctuations of certain instabilities. In the experiment of the Q_T -Upgrade machine [8], segmented plates located at both ends were biased with various voltage levels and the radial potential profile was successfully controlled, although there is no description of biasing effects on the anomalous transport. In the HIEI single mirror device flute mode instability was suppressed using the rf stabilization method [9]. The stability of rotationally driven flute or interchange modes was investigated in Phaedrus by controlling E_r [10]. It was found in this experiment that the rigid $\mathbf{E} \times \mathbf{B}$ rotation was a dominant influence on the observed instability rather than shear in E_r . The experiments of GAMMA 10 [11] revealed that ambipolar potential controlled by biased end rings affects drift wave instability. A gradual change in fluctuation level and radial transport with the bias voltage was observed in corre-

lation with a change in global radial potential profile. These experimental results on mirrors could be explained by a “soft” transition in stability due to a gradual change in rigid rotation of plasma column. Recently, radial transport in a sheared electric field was studied in the PISCES-A linear plasma device [12], and reduction of fluctuation-induced transport was observed. In this experiment, however, no observation of transition or bifurcated phenomena was reported.

This study deals with the improvement on radial confinement using limiter biasing, which is the first observation of H -mode-like behavior in tandem mirrors. With positive limiter biasing, an increase of bulk density and energy, reduction of edge fluctuation level, and steepening of edge density profile are observed. The simultaneous drop of neutral emission and bifurcation of limiter current indicate “hard” transition phenomena. The suppression of edge turbulence may be attributed to the observed rotational shear in the edge.

HIEI [1] is the so-called “ICRF tandem mirror” experimental machine, that is, the tandem mirror operated only by mode-controlled ICRF (ion cyclotron range of frequencies). HIEI has a completely axisymmetric configuration, and the central cell is 1.9 m in length and 25 cm in radius with plug cells 0.7 m in length on both sides of the central cell. The central cell ICRF ($\omega/2\pi=8$ MHz) generates a helicon/fast wave to produce and heat the plasma simultaneously via mode conversion [13]. Ponderomotive force produced by rf field stabilizes the plasma macroscopically against the flute instability [9]. All the measurements described below are performed in HIEI central cell with no axial potential formation. End plates located outside both plug cells are floating. The limiters are located at four axial positions ($z = \pm 18$ cm and ± 34 cm, where z denotes axial position with respect to the midplane of the central cell). Each limiter has a radius $a = 14$ cm (projected to $z = 0$ cm plane) and is segmented into four parts azimuthally. One limiter located at $z = -34$ cm is utilized for biasing by applying dc voltage to four segments in parallel, and the other limiters are floating. The dc power supply is a capacitor bank of $2.8 \times 10^4 \mu\text{F}$ and the voltage between -300 and $+300$ V

with respect to the grounded vessel wall is used for biasing on the limiter in the experiments.

The magnetic field strength at the midplane of the central cell is set to 0.035 T with the mirror ratio 7. Plasma is produced using the central cell ICRF (the net input power = 50–70 kW) with He gas puffing. Hydrogen atoms with a few percents are involved from the wall as recycling particles. The plasma parameters of typical discharges are peak plasma density $n_e \sim 7 \times 10^{12} \text{ cm}^{-3}$ in the case of no biasing on the limiter, $T_e = 10\text{--}30 \text{ eV}$, and $T_i = 30\text{--}40 \text{ eV}$. Plasma line density is measured by a FIR laser interferometer, and local density and density fluctuations in the edge are monitored by Langmuir probes calibrated by the FIR interferometer. T_e and T_i show no significant change by the limiter biasing.

Figure 1 shows the time evolution of, from top to bottom, limiter bias voltage V_{bias} , limiter current I_{bias} , line density nl , stored energy as measured by diamagnetic loop W_{dia} , and neutral line emission (HeI) with (solid line) and without (dotted line) the limiter biasing of $\sim 130 \text{ V}$. Before the limiter biasing for $t < 10 \text{ msec}$, fluctuations with large amplitude are observed at $10 \text{ cm} < r < 13.5 \text{ cm}$ ($0.71 < r/a < 0.96$), i.e., in the plasma periphery. The density and potential fluctuation levels $\tilde{n}/\langle n \rangle$ and $\tilde{V}_f/\langle V_f \rangle$ at $r = 12 \text{ cm}$ are ~ 0.5 and ~ 0.2 , respectively, where n is the local plasma density, V_f is the

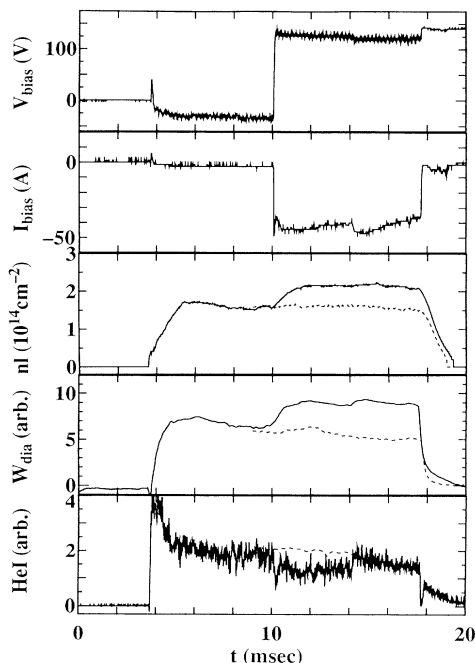


FIG. 1. Typical temporal evolutions of global plasma parameters of a positive bias shot (solid line) in comparison with a no-biasing shot (dotted line). From top to bottom: bias voltage on the limiter V_{bias} , limiter current I_{bias} , line density through the axis ($z = 0 \text{ cm}$) nl , stored energy (diamagnetism) ($z = -60 \text{ cm}$) W_{dia} , and HeI emission through the axis ($z = -30 \text{ cm}$).

floating potential, the tilde denotes the fluctuating part, and angular brackets denote a time average over a time scale long compared to the frequency of the fluctuations. The value of $\tilde{n}/\langle n \rangle$ at $r = 12 \text{ cm}$ (~ 0.5) is larger by a factor of 5–10 than at $r = 0 \text{ cm}$ (< 0.1). The frequency of the fluctuations ranges from $\sim 4 \text{ kHz}$ to $\sim 12 \text{ kHz}$ with the azimuthal mode number 2–6. The fluctuations are inferred to be driven by drift mode instability as described in the following. The fluctuations are localized in the region of steep density gradient. Axial correlation measurement reveals that the instability has a finite value of $k_{\parallel} \sim 0.9 \text{ m}^{-1}$. The propagating direction is inferred to be of the electron diamagnetic drift by a cross-correlation technique. After the onset of limiter biasing at $t = 10 \text{ msec}$, edge fluctuations suddenly vanish within 0.2 msec. Simultaneously nl rises up to approximately 1.5 times the initial value as well as W_{dia} , as shown in Fig. 1. The emission line intensity of HeI (5876 \AA) drops clearly for 4 msec from the onset of biasing. The dotted line of HeI in the case of no biasing indicates the averaged value for clarity. It is found that H_{α} drops as well. Another significant change is found in I_{bias} in Fig. 1. At $t = 10 \text{ msec}$, which corresponds to the starting point of the HeI drop, I_{bias} decreases suddenly (we can recognize it as a small peak in I_{bias} at $t = 10 \text{ msec}$). Then at $t = 14 \text{ msec}$, which corresponds to the ending point of the HeI drop, it jumps up to a higher level again.

The voltage-current characteristic of the limiter is shown in Fig. 2. The floating potential of the limiter is around $\sim -30 \text{ V}$. I_{bias} shows a transition from $\sim 60 \text{ A}$ to $\sim 49 \text{ A}$ at $V_{\text{bias}} \sim 80 \text{ V}$, which represents some bifurcation phenomena. The transition point to a lower current level varies with conditions such as the amount of gas puffing or net power of the central cell ICRF, which are related to the content of neutral particles in the scrape-off layer (SOL). As shown in Fig. 1, density buildup and reduction of edge turbulence are observed in the lower current phase. Earlier studies of electrode biasing [5, 14, 15] show a similar tendency, i.e., low currents in the H mode and high currents in the L mode.

Figure 3 shows the dependence of local density at $r = 0 \text{ cm}$ $n(0)$, W_{dia} , and $\tilde{n}/\langle n \rangle$ at $r = 12 \text{ cm}$ ($r/a = 0.86$)

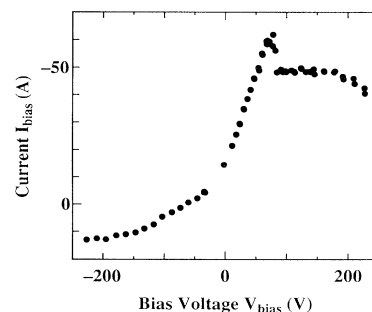


FIG. 2. Voltage-current characteristic of the limiter.

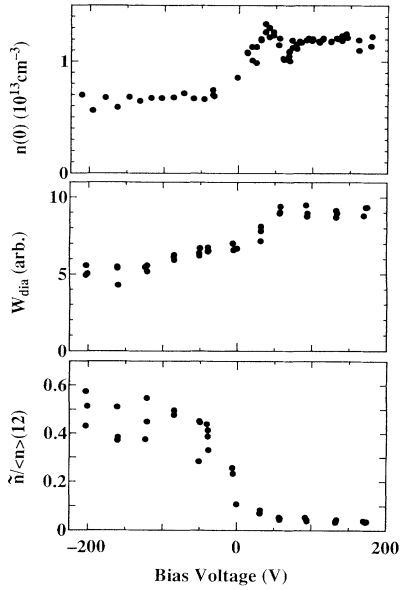


FIG. 3. Density at $r=0$ cm ($z=0$ cm) $n(0)$, stored energy ($z=-60$ cm) W_{dia} , and fluctuation level at $r=12$ cm ($z=0$ cm) $\tilde{n}/\langle n \rangle(12)$ as a function of bias voltage V_{bias} .

$\tilde{n}/\langle n \rangle(12)$ on V_{bias} . As V_{bias} is raised above the floating potential level of the limiter V_{fl} ($V_{\text{fl}} \sim -35$ V in this case), $\tilde{n}/\langle n \rangle(12)$ decreases sharply, which is accompanied by the increase of $n(0)$ as well as W_{dia} . Since T_e is invariant on V_{bias} , the change of W_{dia} reflects that of the global density. nl through the axis rises with V_{bias} as well. $\tilde{n}/\langle n \rangle(12)$ at $r=9$ cm and $\tilde{V}_f/\langle V_f \rangle$ at $r=12$ cm shows the similar variation to $\tilde{n}/\langle n \rangle(12)$ with V_{bias} . The detailed measurement of $\tilde{n}/\langle n \rangle(12)$ by changing V_{bias} in a shot reveals that the fluctuation vanishes at $V_{\text{bias}} - V_{\text{fl}} > 65$ V when V_{bias} increases and that it appears at $V_{\text{bias}} - V_{\text{fl}} < 45$ V when V_{bias} decreases. That is, the hysteresis phenomenon is observed in the stabilization of edge turbulence. This suggests the presence of a non-linear process and some transition phenomena including bifurcation. No significant change is found in all the signals when V_{bias} is varied below V_{fl} .

Figure 4 displays the radial dependence of density and relative angular rotation velocity $\omega_{\theta} (=v_{\theta}/r)$ on V_{bias} . In Fig. 4(a), the increase of density is observed inside the limiter edge, and density in SOL ($r > 11.5$ cm in Fig. 4) shows an abrupt reduction by a factor of 3–5 on the onset of biasing. The E -folding length of radial density gradient in the periphery near the biased limiter changes from ~ 1.5 cm in the case of no biasing to ≤ 0.4 cm in the case of biasing. Such significant modifications of the density profile have not been reported in the dc biasing experiments in other linear devices [10–12]. v_{θ} , shown in Fig. 4(b), is measured as described in the following. The phase difference of \tilde{n} detected by two Langmuir probes separated by 45° in azimuth is converted into velocity us-

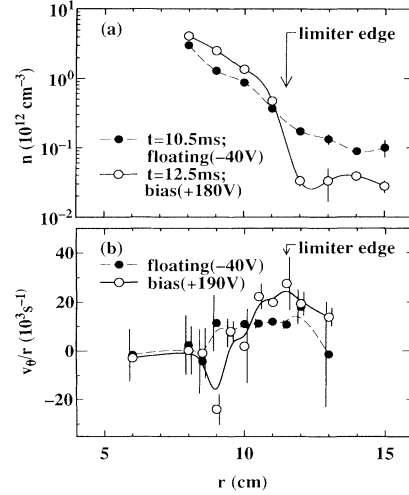


FIG. 4. Radial profile of (a) density and (b) relative angular velocity of plasma rotation in the cases of limiter biasing and no biasing measured at $z=-60$ cm. Bias voltage is applied from $t=11.0$ msec in the case of (a). Note that the radial position of the limiter edge is $r=11.5$ cm at $z=-60$ cm.

ing the relation $v_{\theta} = 2\pi f_d/k_{\theta}$, where $k_{\theta} = m/r$ and f_d is the frequency of the fluctuations. The change of v_{θ} represents approximately that of the $\mathbf{E} \times \mathbf{B}$ rotation velocity since the change of the phase velocity of the instability is relatively negligible. It is evident that, in the case of biasing, rotation becomes more positive ($\omega_{\theta} = v_{\theta}/r \sim 25 \times 10^3 \text{ sec}^{-1}$) at $r > 10.5$ cm than in the case of no biasing ($\omega_{\theta} \sim 10 \times 10^3 \text{ sec}^{-1}$) and that rotational shear with larger amplitude is present in the case of limiter biasing in the region of $9 \text{ cm} < r < 11 \text{ cm}$ than in the case of no biasing. We note that “positive” rotation indicates the rotation in the direction of electron diamagnetic drift. The force balance equation is written

$$E_r = \frac{1}{n_i Z_i e} \frac{\partial P_i}{\partial r} - (\mathbf{v}_i \times \mathbf{B})_r, \quad (1)$$

where n_i , Z_i , and P_i are the ion density, charge, and pressure, respectively. By neglecting the contribution of the ion pressure, E_r in the case of biasing is inferred from the detected azimuthal rotation to be more negative ($\Delta E_r \sim 50$ V/m) at $r > 10$ cm than in the case of no biasing. $|dE_r/dr|$ for $9 \text{ cm} < r < 11 \text{ cm}$ changes roughly by 1 order of the magnitude. No significant change of rotation and E_r for $r < 8$ cm with V_{bias} , i.e., in the bulk region, is found in Fig. 4. The observation of strong rotational shear distinguishes our experiments from those in other mirror devices [10,11]. Similar features, that is, larger E_r and larger rotational shear in the periphery, have been observed in tokamak H -mode discharges [5,6]. The reduction of fluctuations in the edge (see Fig. 3) is attributed to the occurrence of rotational shear, which is theoretically pointed out by Biglari, Diamond, and Terry. Another measurement in terms of dependence of V_{bias} re-

veals that such change of v_θ in the periphery is like a stepwise function on V_{bias} and corresponds to the vanishing of fluctuations in the edge.

Radial particle flux induced by edge turbulence [16], Γ , can be estimated by the correlation between the density fluctuations \tilde{n} and the plasma potential fluctuations $\tilde{\phi}$ over the observed frequency range. The experimental parameters used for the estimations are in the following: $\tilde{n} = 6.0 \times 10^{11} \text{ cm}^{-3}$, $\tilde{\phi} \sim \tilde{V}_f = 6 \text{ V}$, $m = 2-6$ at $r = 0.13 \text{ m}$ ($r/a \sim 0.93$) for the case of no biasing, and $\tilde{n} = 9.0 \times 10^{10} \text{ cm}^{-3}$, $\tilde{\phi} \sim \tilde{V}_f = 1 \text{ V}$, $m = 2$, for the case of biasing. Thus we obtain $\Gamma = 2.2 \times 10^{20} \text{ m}^{-2} \text{ sec}^{-1}$ for the case of no biasing and $\Gamma = 2.8 \times 10^{19} \text{ m}^{-2} \text{ sec}^{-1}$ for the case of biasing. The calculated Γ for the case of no biasing is smaller by 1 order than Γ predicted by Bohm's diffusion and Γ for the case of biasing is larger by a factor of 2 than Γ predicted by the classical diffusion theory. Fluctuation-induced transport decreases with the limiter biasing by 1 order. Figure 3 shows such a tendency clearly; that is, the density due to the reduction of outward fluctuation-induced transport is observed when positive bias voltage is applied to the limiter and the fluctuation is sufficiently suppressed. Γ is connected to the corresponding radial particle confinement time $\tau_{\perp t}$ by the relation $\Gamma 2\pi r = \langle n \rangle \pi r^2 / \tau_{\perp t}$. $\tau_{\perp t}$ in the case of no biasing ($\tau_{\perp t}$) and biasing ($\tau'_{\perp t}$) are estimated using the calculated values of Γ , which yields $\tau_{\perp t} = 0.29 \text{ msec}$ and $\tau'_{\perp t} = 2.8 \text{ msec}$.

nl and W_{dia} rise by the limiter biasing as shown in Fig. 3, and such changes represent the enhancement of particle and energy confinement in the bulk region. The enhancement of radial particle confinement is estimated as follows. The particle balance equation can be written as

$$\frac{dN}{dt} = S - \frac{N}{\tau_{\perp}} - \frac{N}{\tau_{\parallel}}, \quad (2)$$

where N is the global density, S is the fueling rate, and τ is the particle confinement time across/along the magnetic fields. N is estimated from nl , and S is considered to be proportional to the intensity of HeI. We can obtain three equations for (a) the phase before biasing, (b) the density buildup phase just after the onset of biasing, and (c) the steady phase after the buildup phase (see Fig. 1). τ_{\parallel} shows no significant variation with V_{bias} by the measurement of end loss flux. We take $(\tau_{\perp}^{-1} + \tau_{\parallel}^{-1})^{-1}$ before biasing $\sim 0.91 \text{ msec}$ as the decay time of density after switching off the central cell ICRF injection. The value of $(\tau_{\perp}^{-1} + \tau_{\parallel}^{-1})^{-1}$ during HeI drop is calculated as 2.3 msec from Eq. (2). The density exponentiation time in phase (b) in Fig. 1 is $\sim 1.5 \text{ msec}$, which also yields $(\tau_{\perp}^{-1} + \tau_{\parallel}^{-1})^{-1} \sim 2.3 \text{ msec}$. We note that this enhancement of particle confinement time (~ 2.5) is attributed to the improved radial confinement.

The improvement on radial confinement is also verified by the drop of HeI and the shortened radial density decay

length by a factor of 4. That is attributed to the reduction of fluctuation-induced transport and the edge turbulence suppression is inferred to result from rotational shear. The observed rotational shear appears to be formed through bifurcation in rotation velocity that is related to the observed bifurcation in I_{bias} .

In conclusion, we have demonstrated the transition leading to the improved radial confinement induced by dc limiter biasing in the HIEI tandem mirror. As the bias voltage on the limiter is raised in the range of positive values, the fluctuation level of both density and potential in the edge region decreases and the bulk density increases up to $1.2 \times 10^{13} \text{ cm}^{-3}$ by a factor of 1.5-2. The particle confinement time is estimated to increase by a factor of 2.5. During this high radial confinement mode, HeI and H α drop, limiter current decreases, and plasma rotation changes significantly. Radial electric field is inferred to be larger from the rotation measurement and its shear might suppress the edge turbulence. The observed strong nonlinear phenomena, the change of the limiter currents, and the sudden drop of HeI demonstrate the bifurcation feature, which is similar to that in the *L-H* transition in tokamaks.

The authors gratefully acknowledge the hospitality and the help of H. Takeno, M. Shima, and H. Yoshida in the execution of experiments and for useful discussions. This work was supported in part by the Grant in Aid for Scientific Research from the Ministry of Education.

-
- [1] Y. Yasaka *et al.*, in *Plasma Physics and Controlled Nuclear Fusion Research* (IAEA, Washington, 1990), Vol. 2, p. 725.
 - [2] M. Inutake *et al.*, *Phys. Rev. Lett.* **55**, 939 (1985).
 - [3] F. Wagner *et al.*, *Phys. Rev. Lett.* **49**, 1408 (1982).
 - [4] K. C. Shaing and E. C. Crume, Jr., *Phys. Rev. Lett.* **63**, 2369 (1989).
 - [5] R. J. Taylor *et al.*, *Phys. Rev. Lett.* **63**, 2365 (1989); R. R. Weynants and R. J. Taylor, *Nucl. Fusion* **30**, 945 (1990).
 - [6] R. J. Groebner, K. H. Burrell, and R. P. Seraydarian, *Phys. Rev. Lett.* **64**, 3015 (1990); H. Matsumoto *et al.*, *Plasma Phys. Controlled Fusion* **34**, 615 (1992).
 - [7] H. Biglari, P. H. Diamond, and P. W. Terry, *Phys. Fluids B* **2**, 1 (1990).
 - [8] A. Tsushima *et al.*, *Phys. Rev. Lett.* **56**, 1815 (1986).
 - [9] Y. Yasaka and R. Itatani, *Phys. Rev. Lett.* **56**, 2811 (1986).
 - [10] G. D. Severn *et al.*, *Phys. Fluids B* **3**, 114 (1991).
 - [11] A. Mase *et al.*, *Phys. Rev. Lett.* **64**, 2281 (1990).
 - [12] R. J. Taylor *et al.*, in *Plasma Physics and Controlled Nuclear Fusion Research* (Ref. [1]), Vol. 1, p. 463.
 - [13] Y. Yasaka *et al.*, *Phys. Fluids B* **4**, 1486 (1992).
 - [14] L. G. Askinazi *et al.*, *Nucl. Fusion* **32**, 271 (1992).
 - [15] R. R. Weynants *et al.*, *Nucl. Fusion* **32**, 837 (1992).
 - [16] P. C. Liewer, *Nucl. Fusion* **25**, 543 (1985).